

Structure–Property Relationships and $^1\text{O}_2$ Photosensitisation in Sterically Encumbered Diimine Pt^{II} Acetylide ComplexesDeanne Nolan,^[a] Belén Gil,^[a] Longsheng Wang,^[b] Jianzhang Zhao,^[c] and Sylvia M. Draper*^[a]

Abstract: A series of sterically encumbered $[\text{Pt}(\text{L})(\sigma\text{-acetylide})_2]$ complexes were prepared in which **L**, a dendritic polyaromatic diimine ligand, was held constant (**L** = 1-(2,2'-bipyrid-6-yl)-2,3,4,5-tetrakis(4-*tert*-butylphenyl)benzene) and the *cis* ethynyl co-ligands were varied. The optical properties of the complexes were tuned by changing the electronic character, extent of π conjugation and steric bulk of the ethynyl ligands. Replacing electron-withdrawing phenyl- CF_3 substituents (**4**) with electron-donating pyrenes (**5**) resulted in a red shift of both the lowest-energy absorption ($\Delta E = 3300 \text{ cm}^{-1}$, 61 nm) and emission bands ($\Delta E = 1930 \text{ cm}^{-1}$, 64 nm). The emission,

assigned in each case as phosphorescence on the basis of the excited-state lifetimes, switched from being $^3\text{MMLL}'\text{CT}$ -derived (mixed metal-ligand-to-ligand charge transfer) when phenyl/polyphenylene substituents (**3**, **4**, **6**) were present, to ligand-centred $^3\pi\pi^*$ when the substituents were more conjugated aromatic platforms [pyrene (**5**) or hexa-*peri*-hexabenzocoronene (**7**)]. The novel Pt^{II} acetylide complexes **5** and **7** absorb strongly in the visible region of the electromagnetic spec-

trum, which along with their long triplet excited-state lifetimes suggested they would be good candidates for use as singlet-oxygen photosensitisers. Determined by in situ photooxidation of 1,5-dihydroxynaphthalene (DHN), the photooxidation rate with pyrenyl-**5** as sensitizer ($k_{\text{obs}} = 39.3 \times 10^{-3} \text{ min}^{-1}$) was over half that of the known $^1\text{O}_2$ sensitizer tetraphenylporphyrin ($k_{\text{obs}} = 78.6 \times 10^{-3} \text{ min}^{-1}$) under the same conditions. Measured $^1\text{O}_2$ quantum yields of complexes **5** and **7** were half and one-third, respectively, of that of TPP, and thus reveal an efficient triplet–triplet energy-transfer process in both cases.

Keywords: acetylide ligands • chelates • photochemistry • photophysics • platinum

Introduction

Polyphenylenes may be considered to be monodisperse, polyaromatic dendrimers due to their stiff radial arms, stringent geometry and controllable pore size.^[1] Hexaphenylbenzene (HPB) derivatives are a subset of this group and have been applied as host materials for the detection of volatile organic compounds,^[2] (e.g., via a pentaaryl Pt^{II} terpyridyl complex),^[3] in the generation of large-surface support frameworks for multichromophoric arrays^[4] and in artificial photosynthesis.^[5] The functionalisation of sterically demanding polyphenylenes with bipyridyl units has given rise to a variety of shape-persistent coordination complexes in which the rigid polyaromatic dendrons essentially encapsulate the metal centre.^[6]

Numerous polyarylated organometallic compounds have been prepared, including some with bulky substituents that exhibit correlated rotation,^[7] and HPB Pd^{II} pincer complexes that behave as homogeneous Lewis acid catalysts.^[8] The HPBs are interesting synthetic precursors for graphenelike hexa-*peri*-hexabenzocoronene (HBC) platforms,^[9] and π -conjugated transition metal compounds have been extensively investigated as triplet emitters in optoelectronic devices.^[10] Pt^{II} acetylides are particularly viable materials for such applications.^[11] The optical properties of mixed poly-pyridyl metal–alkynyl systems can be tuned by functionalisa-

[a] Dr. D. Nolan, Dr. B. Gil, Prof. S. M. Draper
School of Chemistry, University of Dublin, Trinity College
College Green, Dublin 2 (Ireland)
Fax: (+353)1-6712826
E-mail: smdraper@tcd.ie

[b] Dr. L. Wang
School of Chemical and Chemical Engineering
Ministry of Light Industry, Hubei University of Technology
Wuhan City 430068 (P. R. China)

[c] Prof. J. Zhao
State (National) Key Laboratory of Fine Chemicals
School of Chemical Engineering, Dalian University of Technology
Room E-208 West Campus, Dalian 116024 (P. R. China)

Supporting information for this article is available on the WWW under <http://dx.doi.org/10.1002/chem.201300759>. It contains crystal data and structure refinement details for **2** (Table S1) and **3** (Table S2); ORTEPs of **2** (Figure S1) and **3** (Figure S2); temperature-dependent ^1H NMR spectra of **4** and **5** (Figure S3a, S3b); concentration-dependent ^1H NMR spectra of **3** and **4** (Figure S4a, S4b); concentration-dependent ^1H NMR spectra of **5** (Figure S5); normalised UV/Vis absorption spectra of **L**, **1** and **3** in CH_2Cl_2 (Figure S6); normalised emission spectra of **3**, **4** and **6** in CH_2Cl_2 solution at 298 K [$\lambda_{\text{exc}} < 350 \text{ nm}$ (Figure S7a), $\lambda_{\text{exc}} > 420 \text{ nm}$ (Figure S7b)] and at 77 K (Figure S8); and UV/Vis absorption spectra showing photooxidation of DHN with complex **4** as $^1\text{O}_2$ photosensitiser (Figure S9).

tion of the polypyridyl ligand or by structural modification of the acetylide. The strong spin-orbit coupling of the Pt centre allows for efficient singlet-triplet mixing, which facilitates phosphorescence from the appended chromophore. The strong-field acetylides ensure that non-radiative deactivation of the emissive excited state is less likely.^[12]

Since the first preparation of a diimine Pt^{II} bis-acetylide by Che et al.,^[13] compounds of this class have attracted considerable interest. In 2000, a series of highly emissive Pt bipyridyl bis(aryl acetylide) complexes were reported by Eisenberg et al., in which synthetic variation of the aryl acetylide ligand facilitated a comprehensive investigation into the nature of the excited state.^[14] Concomitant results described by Schanze et al. and separately by Che et al. detailed the influence of changing the electronic demand of the diimine ligand (by varying substituents) on the emission energy.^[15] In both cases, the photophysics of these materials was shown to be dominated by metal-to-ligand charge transfer, ³MLCT [Pt(5d)→π*(N[^]N)]. In contrast, Castellano et al. showed that incorporation of an alkynyl pyrene sensitises room-temperature intraligand phosphorescence (³IL) from the pyrenyl core in fluid solution as a consequence of the heavy-metal effect of the Pt^{II} centre.^[16] Photoinduced intramolecular electron-transfer quenching has also been studied for a series of chromophore-dyad complexes incorporating diimine Pt^{II} acetylide complexes as the chromophoric unit.^[17] Alkynyl Pt^{II} polypyridyl complexes (bipyridyl or terpyridyl) have found application in areas spanning photocatalytic hydrogen production,^[18] vapoluminescent materials,^[19] chromophores in dye-sensitised solar cells^[20] and luminescent labels for bioconjugates,^[21] and some exhibit lamellar liquid-crystalline behaviour and thermoreversible metallogelation.^[22]

The high yield of long-lived triplet excited states (e.g., ³IL) in Pt^{II} and Ir^{III} complexes, a consequence of an efficient intersystem crossing process, has seen them employed as efficient triplet photosensitisers. Alkynyl Pt^{II} polypyridyl complexes have shown application in areas such as photocatalysis^[18b,23] and triplet-triplet energy-transfer (TTET) processes, for example, triplet-triplet annihilation-based upconversion (TTA) and singlet-oxygen sensitisation.^[24] The ability of heavy-metal complexes to sensitise the conversion of triplet oxygen to highly reactive singlet oxygen is under intense scrutiny for several applications, particularly in photodynamic therapy.^[25]

This paper reports a new series of diimine Pt^{II} bis-acetylides in which the diimine ligand is held constant while the electronic character and steric demands of the appended alkynyl chromophores are varied. The series offers an unprecedented increase in the degree of steric encumbrance on the Pt^{II} centre and an opportunity to determine, from an unusual perspective, the optical properties as a function of structure. The bulky diimine 1-(2,2'-bipyrid-6-yl)-2,3,4,5-tetrakis(4-*tert*-butylphenyl)benzene is a polyphenylene bipyridine comprising seven aromatic rings. Its unusual asymmetric design combines functionalized polyaryl substituents with a bidentate diimine moiety. The structural features of the

complexes were established by single-crystal X-ray crystallography and temperature- and concentration-dependent ¹H NMR experiments. Complexation results in encapsulation of the Pt^{II} centre in a rigid, sterically encumbered polyphenylene environment that excludes the possibility of metal-metal bonding interactions.

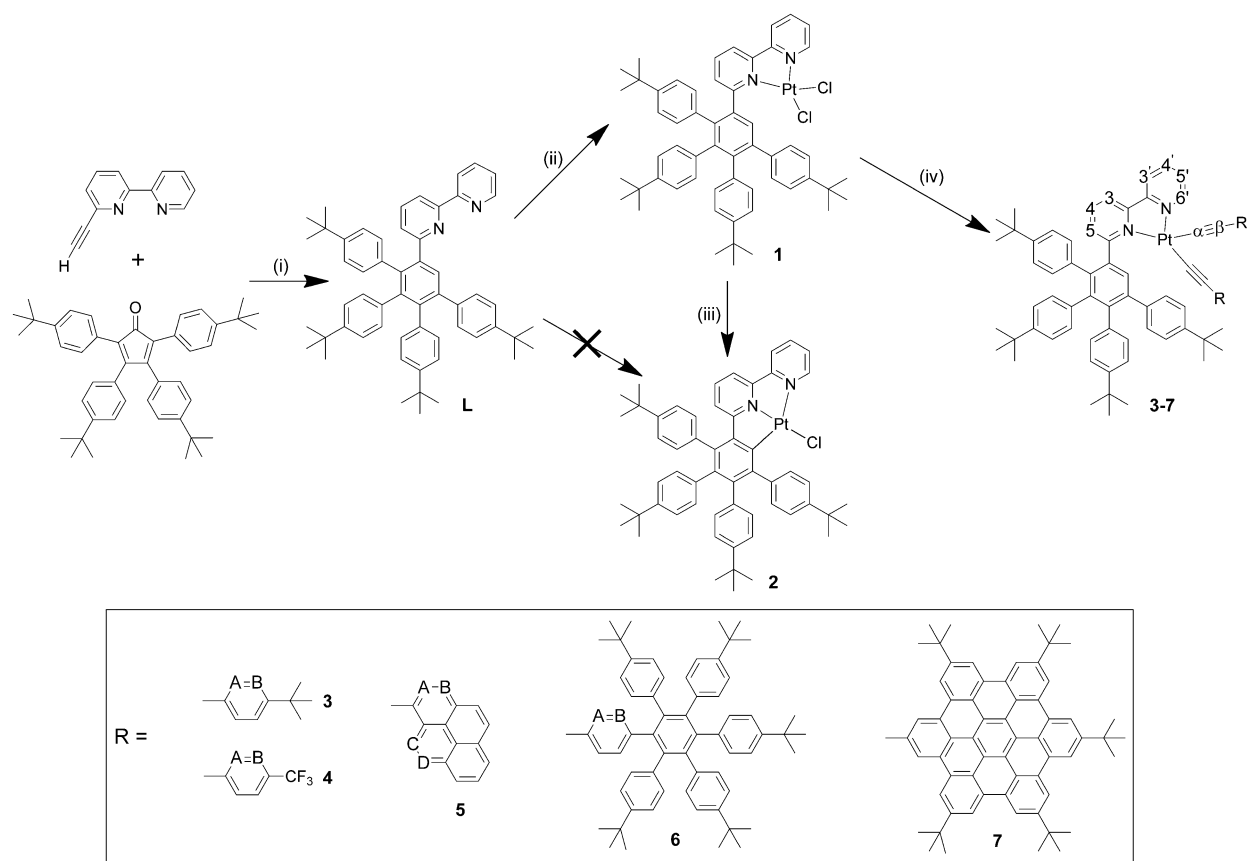
Results and Discussion

Synthesis: The novel ligand 1-(2,2'-bipyrid-6-yl)-2,3,4,5-tetrakis(4-*tert*-butylphenyl)benzene (**L**) was prepared by [2+4] Diels-Alder cycloaddition between 2,3,4,5-tetrakis(4-*tert*-butylphenyl)cyclopenta-2,4-dienone and 6-ethynyl-2,2'-bipyridine (Scheme 1).^[9b,26] Ligand **L** has the potential to coordinate to a metal centre such as Pt in two different modes (Scheme 1), namely, bidentate bipyridyl coordination to yield [Pt(L:N[^]N)Cl₂] (**1**) or, once deprotonated and anionic, by pseudo-terpyridine coordination to yield [Pt(L:N[^]N^{^-}C)Cl] (**2**). The synthesis of **1** was achieved by heating **L** and *cis*-[PtCl₂(DMSO)₂] to reflux in chloroform. In comparison, cyclometallated **2** proved more difficult to prepare in reasonable yield despite attempting multiple synthetic routes. These included using a variety of solvents,^[27] alternative Pt^{II} salts^[28] and preparing a dichloro-bridged Pt^{II} dimer followed by water-induced CH activation.^[29] Complex **2** was eventually isolated in poor yield from a CHCl₃/EtOH solution of **1** on standing. The conversion of diimine-coordinated **1** to cyclometallated **2** was confirmed by ¹H NMR spectroscopy (in particular the absence of a singlet for an H atom on the central phenyl ring of **2**) and single-crystal X-ray diffraction (see below).

The [Pt(L)(C≡CR)₂] complexes **3–7** were prepared by a series of CuI-catalysed, chloride-to-alkyne exchange reactions. The polyphenylene alkyne 1-(4-ethynylphenyl)-2,3,4,5,6-penta-(4-*tert*-butylphenyl)benzene and fully cyclised 2-ethynyl-5,8,11,14,17-penta-*tert*-butylhexa-*peri*-hexabenzocoronene (HBC) were prepared by published procedures.^[30] The steric bulk of these alkynes meant that an excess of alkyne co-ligand and extended reaction times were required.

Complexes **3–6** were fully characterised by NMR spectroscopy (¹H and ¹³C{¹H}), as well as ¹⁹F for **4**), IR spectroscopy, mass spectrometry and elemental analysis. As expected, several of the proton signals of the bipyridyl ligand are affected significantly by the nature of the acetylide and underwent marked shifts upon complexation. Proton H6', which is immediately adjacent to the coordinated nitrogen atom (Scheme 1), has the most-downfield of all the proton signals in each complex; it shifts from δ = 8.60 ppm in **L** to δ = 9.53 ppm for **1** and to δ = 10.26 ppm in **7**.

The poor solubility of **7** precluded the measurement of its ¹³C {¹H} NMR spectrum, but for the other complexes **3–6** two acetylenic ¹³C signals were observed for each acetylide ligand. The ¹³C-¹⁹⁵Pt coupling constants of C_α and C_β were identified by a HMBC experiment on account of the three-bond coupling of H_A (the CH signal closest to the C≡C moiety) to C_β on each acetylide (Scheme 1).



Scheme 1. Synthesis of bipyridyl ligand **L**, Pt^{II} chloride precursor **2** and alkynyl complexes **3–7**. i) Benzophenone, 150–200 °C, 6 h, 84%; ii) *cis*-[PtCl₂(DMSO)₂] (1 equiv), CHCl₃, 55 °C, 48 h, 77%; iii) C₂H₅OH/CHCl₃, 7%; iv) Aryl acetylene (2 equiv), CH₂Cl₂, *i*Pr₂NH, CuI (cat.); **3** 62%, **4** 55%, **5** 31%, **6** 29%, **7** 77%.

For each member of the family of compounds [Pt(**L**)(C≡CR)₂] (**3–7**), the asymmetric diimine ligand results in chemically inequivalent acetylide co-ligands giving rise to two ν(C≡C) infrared stretching bands with values in good agreement with those obtained for analogous complexes.^[14,31]

Variable-temperature/concentration ¹H NMR spectroscopy:

The ¹H NMR spectrum of **1** is complex due to both the asymmetric nature of **L** and the steric constraints within the molecule. Free rotation is sufficiently slowed on the NMR timescale to broaden the proton signals, and some of the phenyl ring protons, which should yield two linked doublets in an AB substitution pattern, appear as four separate phenyl proton resonances. This effect is more apparent in alkynyl complexes **3–7** and was investigated by temperature-dependent ¹H NMR experiments (20–100 °C, [D₆]DMSO). On increasing the temperature, the signals due to the *tert*-butyl-substituted phenyl ring protons sharpen to give rise to fewer and more-resolved doublets, which are shifted downfield (e.g., see spectra for CF₃-containing complex **4** in Supporting Information Figure S3a). This is indicative of increased rotational motion, as geometrically equivalent protons become magnetically equivalent on the ¹H NMR timescale. This high degree of intramolecular steric constraint

persists in complexes **3–6**, as evidenced by variable-temperature ¹H NMR experiments. Interestingly, the additional steric bulk of pyrenyl-bearing **5** appears to give rise to even more restricted internal rotation than in **3**, **4** and **6**. By 90 °C (Supporting Information Figure S3b), several of the proton ring signals have coalesced to very broad featureless signals between δ = 5.9 and 6.8 ppm but have not yet sharpened; more energy (i.e., higher temperature) is required for the molecule to cross the rotational barrier imposed by steric congestion.

To investigate the effect of intermolecular aggregation, concentration-dependent NMR studies were carried out over the range 0.1–10 mM (for compounds **1** and **3–6**, poor solubility of **7** precluded its measurement, except at very low concentrations). For compounds **1**, **3**, **4** and **6**, only very slight changes under these conditions were observed [i.e., up to a maximum of 0.05 ppm downfield shift from 0.1 to 10 mM; Supporting Information Figures S4a (**3**) and Figure S4b (**4**)]. Pyrenyl-containing complex **5**, studied over the range of 0.1 to 10 mM, exhibited different behaviour (Supporting Information Figure S5). Between δ = 7.8 and 10.3 ppm (Supporting Information Figure S5b), a gradual downfield shift of the aromatic proton signals occurred (e.g., the doublet centred at δ = 10.15 ppm). It appears that the

^1H NMR spectroscopic properties of **5** are influenced both by intramolecular steric encumbrance and, in contrast to **1**, **3**, **4** and **6**, some intermolecular aggregation. This feature was investigated further in a subsequent photophysical investigation.

In combination with the crystal structure of **3** (see below) we concluded that the interactions causing the restricted movements in **1**, **3**, **4** and **6** are predominantly intramolecular. In these cases, the influence of intermolecular interactions on the observed NMR spectra and consequent optical properties is minimal.

X-ray crystallography: $[\text{Pt}(\text{L}:\text{N}^{\wedge}\text{N}^{\wedge}\text{C})\text{Cl}]$ (**2**) was obtained as fine orange needles from a solution of **1** in chloroform/ethanol on standing. It crystallised in monoclinic space group $C2/c$ with one molecule of **2** and one water molecule in the asymmetric unit (Supporting Information Figure S1). The geometry about the Pt centre is distorted square-planar (C1-Pt1-Cl1 $105.6(9)^\circ$; N1-Pt1-C1 $76.7(1)^\circ$) and deviates slightly from those typically determined for $\text{N}^{\wedge}\text{N}^{\wedge}\text{C}/\text{Pt}^{\text{II}}$ systems (C-Pt-Cl ca. 100° , N-Pt-C ca. 82°)^[32] due to the steric demands of the $[\text{N}^{\wedge}\text{N}^{\wedge}\text{C}]$ pseudo-terpyridine and its extended substituents (e.g., ring G in Figure 1a). The $[\text{N}^{\wedge}\text{N}^{\wedge}\text{C}]$ ligand moiety is almost planar, with tilt angles of 10.8 and 11.9° for rings B and C, with respect to the plane of the central phenyl ring A (Table 1). The four propeller-like phenyl

Table 1. Tilt angles made between the central ring A and the peripheral aromatic rings in **2** and **3**. Rings are identified by a letter according to Figures 1 and 2.

	Tilt angle with respect to ring A [$^\circ$]
2	B: 10.8 ; C: 11.9 ; D: 73.8 ; E: 85.8 ; F: 79.4 ; G: 75.3
3	B: 54 ; C: 49 ; D: 62 ; E: 66 ; F: 62 ; G: 55

substituents twist at angles between 73.8 and 85.8° from the plane of ring A.^[30b,33] Pyridine ring C is involved in an offset, face-to-face π -stacking interaction with pyridine ring B on an adjacent molecule and this gives rise to head-to-tail dimeric pairs in the crystal lattice (Figure 1 b).

Yellow needles of **3** suitable for single crystal X-ray crystallography were grown from a CH_2Cl_2 solution layered with methanol. Complex **3** crystallises in the tetragonal space group $I4_1/a$, and the asymmetric unit contains one molecule of **3** (Figure 2), one molecule of methanol and three water molecules. Unfortunately, poor crystal quality, despite extensive consequent refinement, precludes very detailed discussion of the structure. As for **2**, the geometry of the Pt^{II} centre can be described as distorted square-planar, but in this case the steric bulk of the substituents combines to push the acetylide ligands closer together. As a result, the bite angles of the ligands about the metal centre deviate from those of similar systems in the literature: the C9-Pt1-C7 bond angle of 85° is slightly smaller and the N2-Pt1-C9 angle of 100° slightly larger than expected (standard ranges: $89\text{--}94$ and $94\text{--}97^\circ$ respectively).^[19a,31,34] The bulky diimine

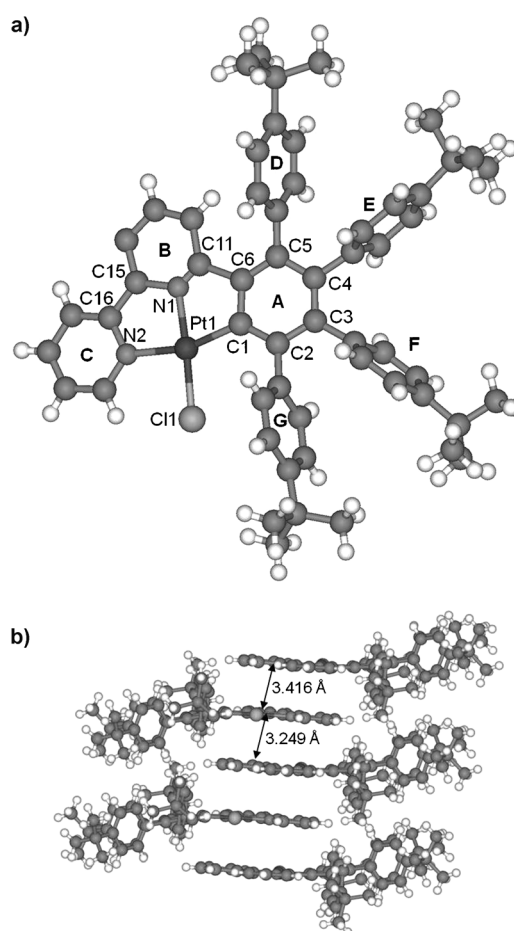


Figure 1. a) Perspective view of **2** with selected atom numbering and ring labelling. b) Packing arrangement of **2** viewed down the c axis. Distances are measured from N1 and the centroid of ring C on an adjacent molecule. Solvent molecules have been removed for clarity. Selected bond lengths [\AA] and angles [$^\circ$]: Pt1-C1 $2.008(2)$, Pt1-N2 $2.112(2)$, Pt1-N1 $2.044(3)$, Pt1-Cl1 $2.319(10)$; C1-Pt1-N1 $76.7(11)$, N1-Pt1-N2 $84.9(10)$, C1-Pt1-Cl1 $105.6(9)$, N2-Pt1-Cl1 $92.9(8)$.

causes the ethynyl moieties, particularly Pt1-C9-C10 , to deviate quite significantly from linearity (169°), and the phenyl rings of the acetylide ligands are similarly forced to tilt out of the Pt^{II} coordination plane.

A significant degree of steric strain is evident in the solid-state structure of **3**. For example, the distances between phenyl acetylide C76 and C36 on ring F and between phenyl acetylide C72 and C26 on ring E are both only slightly larger than the sum of the van der Waals radii of two carbon atoms (3.40 \AA). Such short contact distances would suggest reduced rotational freedom in these phenyl rings and are consistent with the temperature dependence and unusual features in the ^1H NMR spectrum.

UV/Vis absorption spectra: The absorption spectra of ligand **L** and complexes **1** and **3–7** were recorded (Table 2). Diimine ligand **L** shows the broad and featureless absorption spectrum typical of a non-planar polyphenylene and is composed of high-energy ($\lambda = 200\text{--}320 \text{ nm}$) ligand-centred $\pi\text{--}\pi^*$

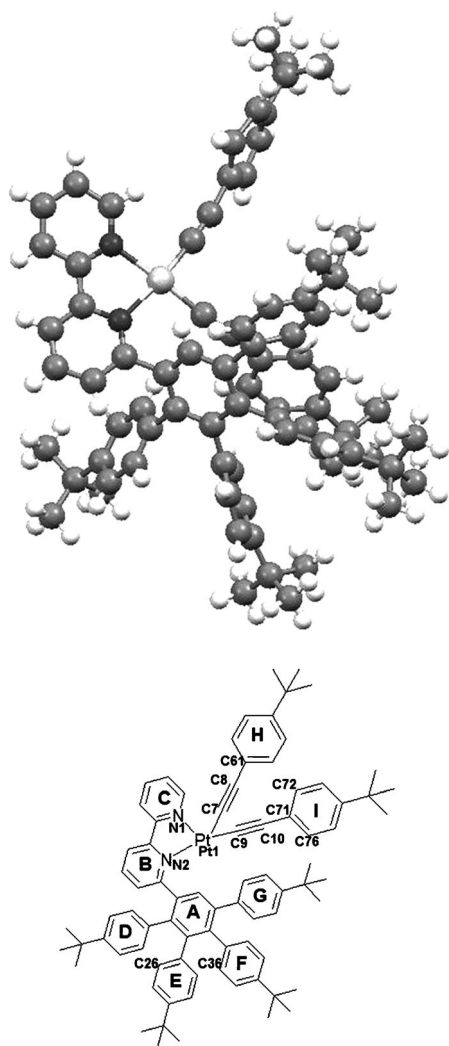


Figure 2. Perspective view of **3** and diagram showing selected atomic numbering and aromatic-ring labelling. Solvent molecules have been removed for clarity.

and $n\text{-}\pi^*$ transitions (Supporting Information Figure S6).^[35] Coordination to the Pt^{II} centre in the form of [Pt-

(L:N^N)Cl₂] (**1**) introduces new bands at 337 and 380 nm and are attributable to metal-to-ligand charge transfer (¹MLCT) [d(Pt)→ $\pi^*(\text{N}^{\wedge}\text{N})$] with some contribution from ³MLCT. The additional weak shoulder at 481 nm ($\epsilon = 0.02\text{ M}^{-1}\text{ cm}^{-1}$) originates from a metal-centred (MC) transition and is a common feature of the absorption spectra of similar [Pt(bpy)Cl₂] (bpy = 2,2'-bipyridine) systems (Supporting Information Figure S6).^[12,36]

The photophysical properties of the acetylide complexes are best considered in two groups: **5** and **7**, and **3**, **4** and **6**. Complexes **5** (ethynyl-pyrene) and **7** (ethynyl-HBC), which contain extended alkynyl π -conjugated platforms, have well-resolved, highly structured absorption bands arising from the $\pi\text{-}\pi^*$ transitions on the appended planar chromophores (Figure 3). The shape of these bands is typical of their re-

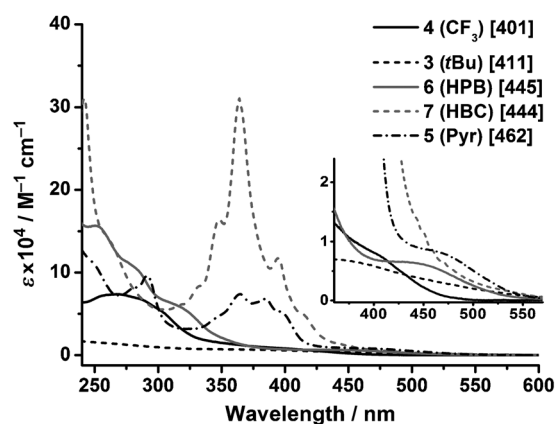


Figure 3. Normalised UV/Vis absorption spectra of complexes **3–7** in CH₂Cl₂ (10⁻⁵ M). Inset: lowest-energy absorption band.

spective chromophore, although they are slightly red-shifted, a consequence of σ donation from the acetylide onto the Pt^{II} centre. In the case of **7**, the additional low energy band at 414 nm probably has some Pt-perturbed intraligand character and some charge-transfer contribution. This band was also observed recently in the absorption spectra of both a

Table 2. Room-temperature UV/Vis spectral data (CH₂Cl₂, $\approx 10^{-5}$ M) and electrochemical data^[a] for diimine ligand L, [Pt(L:N^N)Cl₂] (**1**) and related acetylide complexes [Pt(L:N^N)(C≡CR)] (**3–7**).

	λ_{max} [nm] ($10^{-4}\epsilon \times [\text{M}^{-1}\text{ cm}^{-1}]$)	$E_{\text{pa}}^{\text{ox}}(\text{Pt}^{\text{II}}\text{-Pt}^{\text{III}})$ [V] ^[b]	$E_{\text{pa}}^{\text{ox}}(\text{N}^{\wedge}\text{N}/\text{C}\equiv\text{CR})$ [V] ^[b]	$E_{1/2}^{\text{red}}(\text{N}^{\wedge}\text{N}/\text{C}\equiv\text{CR})[\text{V}]$ ($\Delta E_{\text{p}} [\text{mV}]$) ^[d]
1	234 (5.3), 250 (5.1), 279 (3.8), 304 sh (2.2)	–	+1.07	–1.96 (273) ^[c]
3 (tBu)	250 (5.6), 278 (4.6), 337 (1.6), 380 (0.8), 418 sh (0.3), 481 (0.02)	+0.70	+1.01	–1.74 (169)
4 (CF ₃)	261 (8.9), 292 sh (5.8), 356 (1.6), 411 (0.7)	+0.56	+1.01	–1.90 (101)
5 (Pyr)	257 (7.3), 267 (7.4), 283 (7.0), 302 sh (5.4), 357 (1.4), 401 (0.8)	+0.87	–	–1.85 (191)
6 (HPB)	232 (14.4), 248 sh (11.3), 280 (8.1), 291 (9.6), 347 sh (4.7), 364 (7.4), 384 (6.9), 397 (5.2), 462 (0.8)	+0.37	+0.83	–1.86 (85)
7 (HBC)	251 (15.7), 279 (10.9), 313 (6.1), 445 (0.6)	+0.58	–	–1.92 (104), –2.20 (43)
	231 (34.8), 241 (31.0), 260 (14.3), 317 (6.1), 332 (8.3), 348 (16.5), 364 (31.0), 395 (11.7), 414 (5.0), 445 (1.4)	+0.45	+0.80	–1.90 (81)

[a] In deoxygenated dichloromethane (0.1 M, *n*Bu₄NPF₆) at 298 K, scan rate = 100 mV s⁻¹, versus Fc/Fc⁺. [b] Irreversible/quasi-reversible oxidation process, $E_{\text{pa}}^{\text{ox}}$ (anodic peak potential) quoted. [c] Return oxidation wave associated with this reduction is poorly defined. [d] $\Delta E_{\text{p}} = E_{\text{pa}} - E_{\text{pc}}$, peak potential separation.

cis and a *trans* Pt^{II} phosphine complex containing two ethynyl-HBC ligands.^[30b]

The most significant feature in the spectra of complexes **3**, **4** and **6** is a low-energy absorption band that is red-shifted with increasing electron-donating character of the acetylide.^[14,15,37] This low-energy band, which is absent in **L** and Pt^{II} precursor **1** and buried for the most part under the PAH absorption bands in **5** and **7**, appears at highest energy in **4** ($\lambda = 401$ nm), at 411 nm in **3** and at 445 nm for complex **6**. The band is particularly sensitive to the polarity of the solvent and exhibits a significant degree of negative solvatochromism suggesting considerable involvement of charge transfer (e.g., in **6** the band occurs at 472 nm in toluene and 421 nm in acetonitrile).^[12] The close electronic coupling of the acetylide and 5d Pt metal orbitals in **3**, **4** and **6** means that the HOMO is most likely composed of a mixture of both Pt 5d and C≡CR π orbitals. The HOMO–LUMO transition is probably best described as metal-perturbed (mixed metal–ligand)-to-ligand charge transfer MMLL/CT [Pt(d)/ π -(C≡CR)→ π^* (N^N)].^[28,38] A series of Pt^{II} diimine dithiolate complexes in which the electronic demand of both diimine and dithiolate have been varied independently showed similar behaviour.^[39]

Electrochemical properties: Cyclic voltammetric studies were carried out on 1 mM solutions of **L** and complexes **1** and **3–7** in CH₂Cl₂ containing 0.1 M *n*Bu₄PF₆ as electrolyte (Table 2). In all six Pt^{II} complexes the first oxidation process is a quasi-reversible/irreversible oxidation wave between +0.37 and +0.87 V (Table 2), typical of the oxidation of Pt^{II} to Pt^{III}.^[40] The metal-centred oxidation was most difficult in **4** (CF₃) and easiest in **5**, and this corresponds to the change in the electron density on the metal as a result of the electron-donating ability of the acetylide. For complexes **3**, **4** and **6**, the trend observed in the UV/Vis spectrum holds: the Pt^{II} centres in complexes **3** and **6** are significantly easier to oxidise than that of **4**.

In **7**, the Pt^{II}/Pt^{III} oxidation process is coincident with the irreversible first oxidation on the HBC platform, and thus a broadened and unstructured reverse wave arises.^[30b] In general the second quasi-reversible/irreversible oxidation observed in each complex corresponds to the oxidation of **L** or the alkyne and occurs between +0.80 and +1.07 V. One reduction process occurs within the solvent window; it is localized on the diimine ligand and appears at less negative potentials in the complexes than in the free ligand (Table 2).

The dependence of the Pt^{II} oxidation on the alkynyl co-ligand substituent agrees with the red shift of the lowest-energy band in the UV/Vis absorption spectra on going from electron-withdrawing to electron-rich substituents. It is also further evidence of the participation of both the C≡CR π and Pt 5d orbitals in the HOMO of compounds **3**, **4** and **6** and the assignment of the lowest-energy transition in these cases as MMLL/CT.

Emission spectroscopy: The results of the photophysical measurements, including excited-state lifetimes and quan-

tum yields, of compounds **L**, **1** and **3–7** in the solid state and in CH₂Cl₂ solution (298 and 77 K) are summarised in Table 3.

Upon excitation at high energy ($\lambda_{\text{exc}} = 315$ nm), the emission of **L** is dominated by an intense, high-energy band centred at 365 nm (solid state)/ 375 nm (solution), with excited-state lifetimes in the nanosecond region (Table 3, Figure 4).

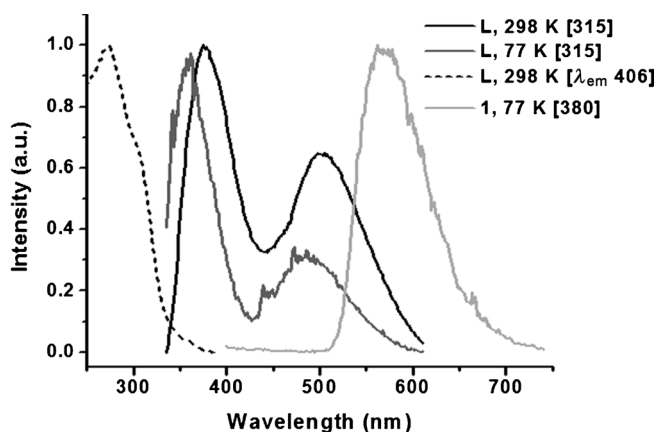


Figure 4. Normalised emission spectra of **L** and [Pt(**L**)Cl₂] (**1**) and excitation spectrum of **L** in CH₂Cl₂ solution at 298 and 77 K [λ_{exc} /nm].

The small Stokes shifts between the lowest-energy excitation band and onset emission and the short lifetimes allow this emission to be assigned as fluorescence from the bipyridine chromophore (¹ $\pi\pi^*$). An additional lower-energy emission band is also evident in the spectrum (507 nm in solution), which has a similar lifetime. These bands feature in the emission spectra of all Pt^{II} complexes of **L** in this work and are characteristic of polyphenylene/bipyridine derivatives in general.^[30b,41]

As is typical of [Pt(bpy)Cl₂]-derived systems, complex **1** is essentially non-emissive as a result of facile non-radiative decay via low-lying d–d excited states and exhibits extremely weak ligand-centred fluorescence ($\lambda = 353$ nm). However, at 77 K in frozen CH₂Cl₂, an intense, broad, structureless emission band is observed at $\lambda_{\text{max}} = 566$ nm, significantly red-shifted from bipyridine-related luminescence bands (Figure 4). This is tentatively assigned to a mixture of ³MLCT and ³d–d.^[12,36]

The photoluminescence data measured for complexes **3–7** are detailed in Table 3 and, as for the UV absorption spectral data, are divided into two groups of compounds according to their analogous photophysical behaviour, that is, complexes **3**, **4** and **6** are considered separately to **5** and **7**.

Complexes 3, 4 and 6 (³MMLL/CT): The solid-state emission spectra of **3**, **4** and **6** at 298 K (Figure 5, top) are dominated by a broad, structureless emission, which shows red shifts in the order **6** > **3** > **4**. Complex **4** containing an electron-withdrawing CF₃-substituted acetylide has the most blue shifted emission ($\lambda_{\text{max}}^{\text{em}} = 524$ nm) and **3** and **6** show red shifts as the acetylide gains more electron-donating charac-

Table 3. Emission data for **L**, [Pt(L)Cl₂] (**1**) and complexes **3–7** in the solid state and in solution (CH₂Cl₂) at 298 and 77 K.

	Medium (<i>T</i> [K])	λ_{em} [nm] (λ_{exc} [nm])	τ [ns] ($\lambda_{\text{exc}}/\lambda_{\text{em}}$ [nm]) ^[b]	Φ_{em}
L	solid (298)	365 _{max} , 512 (315)	39 (295/365), 1010 (370/512)	
	solid (77)	360 _{max} , 508, 554 _{sh} (300)		
	CH ₂ Cl ₂ (298) ^[a]	375 _{max} , 502 (315), 477, 487, 497, 507 _{max} , 531 _{sh} (368)	11 (295/375), 18 (370/504)	< 10 ⁻³ [f]
	CH ₂ Cl ₂ (77)	358 _{max} , 490 (315)		
1	solid (298) ^[c]	non-emissive	non-emissive ^[c]	
	solid (77) ^[c]	362 _{wk} (310)		
	CH ₂ Cl ₂ (298) ^[a,c]	353 _{wk} (290)	poorly emissive ^[c]	< 10 ⁻³ [g]
	CH ₂ Cl ₂ (77)	360 _{wk} , 566 _{max} , 627 _{sh} (309)		
3	solid (298)	358 _{wk} , 543 _{max} (316)	1600 (370/543)	0.016 ^[g]
	solid (77)	537 _{max} , 574 (360)	16 (295/373)	
	CH ₂ Cl ₂ (298) ^[a]	357, 375, 386 _{sh} , 502, 604 _{max} (325), 476, 487, 496, 508, 604 _{max} , 668 _{sh} (425)	134 (13%), 20 (87%) (370/500) 647 (370/600)	
	CH ₂ Cl ₂ (77)	360 _{wk} , 517 _{max} , 542 _{sh} , 572 _{sh} (290–390)		
4	solid (298)	362 _{wk} , 524 _{max} , 561 _{sh} (315)	2100 (370/524)	
	solid (77)	488, 524, 559 _{sh} (360)		
	CH ₂ Cl ₂ (298) ^[a]	355, 374, 387 _{sh} , 476 _{sh} , 533 _{max} (360), 477, 487, 508, 545 _{max} , 607 _{sh} (425)	19 (370/476) 363 (24%), 19 (76%) (370/506), 702 (89%), 39 (11%) (370/550)	0.017 ^[g]
	CH ₂ Cl ₂ (77)	363 _{wk} (295), 480 _{max} , 514, 545, 592 _{sh} (400)		
6	solid (298)	361 (305), 599 _{max} (470)	1800 (370/599)	
	solid (77)	360 _{wk} (295), 600 _{max} , 647 (482)		
	CH ₂ Cl ₂ (298) ^[a]	395 _{max} , 413, 472, 502, 609 (345) 477, 496 _{sh} , 506, 609 _{max} , 661 _{sh} (434)	18 (370/473) 19 (84%), 241 (16%) (370/502) 484 (370/609)	0.076 ^[g]
	CH ₂ Cl ₂ (77)	365 _{wk} , 541 _{max} (300), 539 _{max} , 578 _{sh} , 613 _{sh} (440)		
5	solid (298) ^[d]	360 (310)	poorly emissive ^[d]	
	solid (77) ^[d]	355 _{wk} (310)	poorly emissive ^[d]	
	CH ₂ Cl ₂ (298) ^[a] 10 ⁻⁵ M	395, 415, 449 _{max} , 478, 495 _{sh} , 644 _{sh} , 663, 679 _{sh} (360)	9 (370/448), 23 (370/477), 4650 (370/661)	0.042 ^[g]
	CH ₂ Cl ₂ (298) ^[a] 10 ⁻³ M CH ₂ Cl ₂ (77)	662 _{max} , 719, 738 _{sh} (545) 484, 501, 540 _{sh} , 660, 674 _{sh} , 715, 734 (448)	730 (370/662)	
7	solid (298) ^[d]	372 (312), 472, 493, 593 (360)	poorly emissive ^[d]	
	solid (77) ^[d]	367 (309), 558, 583 _{max} , 638 (390–505)	poorly emissive ^[d]	
	CH ₂ Cl ₂ (298) ^[a]	452 _{sh} , 473 _{max} , 481 _{sh} , 491, 501, 525, 536, 545 _{sh} , 560 ^[e] (360)	18 (370/475), 20 (370/504)	0.077 ^[g]
	CH ₂ Cl ₂ (77)	477, 509, 524 _{sh} , 551 _{sh} , 572 _{max} , 618, 630 _{sh} , 667 _{sh} (402)		

[a] Argon-degassed solution, 10⁻⁵ M. [b] Estimated error less than $\tau \pm 10\%$; [c] Very weakly emissive in solid state and in solution (298 K). [d] Poorly emissive in solid state. [e] Tail of emission band extends to 700 nm. [f] Measured with quinine sulfate as a standard, based on three repeat measurements.^[45] [g] Measured with 4',6'-diamidino-2-phenylindole dihydrochloride (DAPI) as a standard, based on three repeat measurements.^[46]

ter (**3** (*t*Bu): $\lambda_{\text{max}}^{\text{em}} = 543$ nm; **6** (HPB): $\lambda_{\text{max}}^{\text{em}} = 599$ nm). The excited-state lifetimes of all three complexes are similar (1.0–2.1 μs , solid state, 298 K). At low temperature, the emission profiles become asymmetric and sharper than at room temperature (Figure 5, bottom), and each has a degree of vibronic fine structure that reveals the magnitude of involvement of the diimine ligand (N=C, C=C) in the emissive excited state (e.g., **4**: $\tilde{\nu}_{(\text{C}=\text{C}/\text{C}=\text{N})} = 1298$ cm⁻¹).

In optically dilute, degassed CH₂Cl₂ solution (298 K), several emissive states are evident for complexes **3**, **4** and **6** (Supporting Information Figure S7a and S7b). In addition to the lower-energy bipyridine-based emission, high-energy ¹IL fluorescence is seen at 360 nm. In the case of polyphenylene complex **6**, intraligand fluorescence (with short nanosecond

lifetimes, Table 3) derived from the hexaphenylbenzene core dominates the spectrum (upon excitation at low energy). The most significant and lowest-energy emission band shifts to lower energy, from $\lambda = 545$ nm (**4**) to $\lambda = 604$ nm (**3**) and to $\lambda = 609$ nm (**6**). The long excited-state lifetimes (e.g., **3**: $\tau = 647$ ns) and large Stokes shifts of this emission suggests it is triplet in origin. The lifetime for **4** at $\lambda = 550$ nm fits two components [$\tau = 702$ ns (89%), $\tau = 39$ ns (11%)], and this suggests the presence of two energetically close emissive states, most likely due to partial overlap of the lower-energy bipyridine emission and the metal-influenced phosphorescent band. The emission maxima undergo large rigidochromic shifts and profile sharpening on lowering the temperature to 77 K; for example, in **3** a shift of $\Delta E_s = 2675$ cm⁻¹

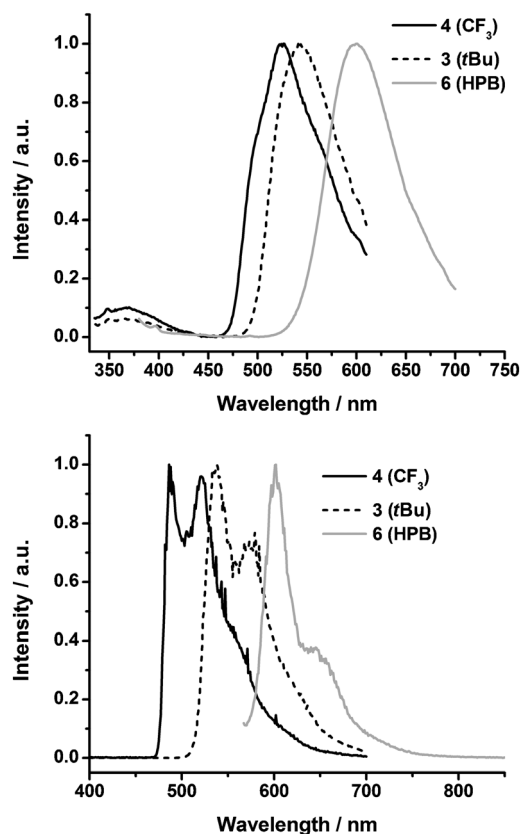


Figure 5. Normalised solid state emission spectra of **3**, **4** and **6**. Top: 298 K (λ_{exc} : **3**, 315 nm; **4**, 316 nm; **6**, 380 nm). Bottom: 77 K (λ_{exc} : **3**, 360 nm; **4**, 360 nm; **6**, 547 nm).

was measured (Figure S8). These large thermally induced Stokes shifts are characteristic of charge transfer emission.^[42]

The decrease in emission energy with increasing electron-donating power of the acetylide co-ligand is a consistent feature of the spectra obtained in the solid state, in solution, and at room and low temperature. This fact, along with the UV/Vis data and electrochemical measurements, reaffirms the assignment of the lowest-energy transition as MMLL/CT [Pt(d)/ $\pi(\text{C}\equiv\text{CR})\rightarrow\pi^*(\text{N}^{\wedge}\text{N})$].

Complexes 5 and 7 ($^3\pi\pi^*$): In contrast to complexes **3**, **4** and **6**, complexes **5** and **7** are essentially non-emissive in the solid state at 298 K and at 77 K. This can be attributed to quenching of the luminescence due to aggregation (e.g., π - π stacking) of the extended alkynyl π -conjugated platforms. In argon-degassed, optically dilute (10^{-5} M) CH_2Cl_2 solution at room temperature, the spectra of **5** and **7** are dominated by emission from their respective highly conjugated aromatic co-ligands. In each case these exhibit an extended emission band with a complex vibronic structure (Figure 6). The emission spectrum of **7** is very similar to that recorded for the free ethynyl-HBC ligand.^[30b] The onset of luminescence occurs at 473 nm and extends to 700 nm. With excited-state lifetimes in the nanosecond region (Table 3), this band can

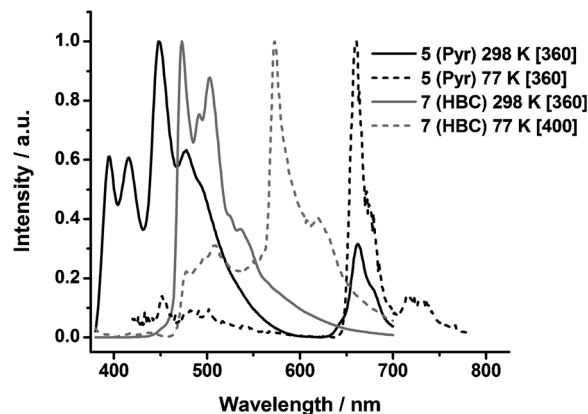


Figure 6. Normalised emission spectra at 298 and 77 K of **5** and **7** in CH_2Cl_2 solution (10^{-5} M) (λ_{exc} [nm]).

be assigned as $^1\pi\pi^*$ based on the hexa-*peri*-hexabenzocorone chromophore.^[43] There is no evidence of the narrow-bandwidth phosphorescence ($^3\pi\pi^*$) at 578 nm that has been shown to be a feature of Pt^{II} acetylide HBC complexes.^[30b,43,44] However, in the case of pyrenyl complex **5**, the lowest-energy band in the emission spectrum (663 nm) has a lifetime of 4.65 μs . In combination with the profile of emission from this complex, this transition can be assigned as phosphorescence originating from a triplet intraligand state on the pyrene chromophore [$^3\pi\pi^*(\text{C}\equiv\text{C-Pyrene})$].^[16] The highest quantum yields of this family of complexes are recorded for **5**, **6** and **7** ($\Phi_{\text{em}}=4.2$, 7.6 and 7.7%, respectively). This is a result of the intense polyaromatic-platform-centred fluorescence and phosphorescence observed for these complexes.

At 77 K in frozen CH_2Cl_2 , intraligand phosphorescence, based on the π -conjugated aromatic co-ligands, dominates the emission spectra of **5** and **7** (Figure 6). Complex **7** displays a narrow-bandwidth emission centred at 577 nm and a shoulder at 618 nm. This corresponds to a triplet excited state localised on the HBC platform, $^3\pi\pi^*(\text{C}\equiv\text{C-HBC})$. Similarly, $^3\pi\pi^*$ phosphorescence from the pyrene chromophore occurs at 660 nm. The extremely small thermally induced Stokes shift (**5**: $\Delta E_s=69\text{ cm}^{-1}$) confirms that emission from **5** and **7** is not derived from a charge-transfer excited state and instead falls within the range expected for a $^3\pi\pi^*$ emissive state.^[16,37b]

The self-quenching of luminescence from complexes **5** and **7** in the solid state prompted us to perform measurements on a solution of **5** in CH_2Cl_2 at higher concentration (solubility issues precluded a similar study on **7**). In 10^{-3} M solution, all of the fluorescence from the pyrene-acetylide chromophore has been quenched (Table 3), leaving solely $^3\pi\pi^*$ phosphorescence from the pyrenyl chromophore. A noticeable decrease in phosphorescence lifetime is also evident (0.73 μs), but no concentration effects are seen in the corresponding UV/Vis spectrum. It can be concluded that, at higher concentrations, pyrenyl-bearing complex **5** self-quenches in solution, most likely by stacking of pyrene chromophores, similar to that observed in concentration-depend-

ent ¹H NMR spectroscopy. This aggregation has little effect on the electronic structure of the triplet excited state, but it does result in a shortening of the excited-state lifetime, similar to that observed elsewhere for Pt^{II} HBC acetylide complexes.^[43]

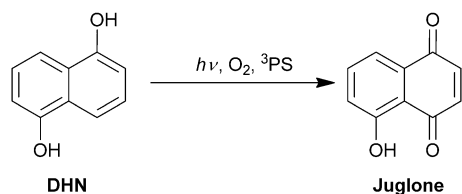
The photoluminescence of complexes **5** (Pyr) and **7** (HBC) is independent of the coordinated diimine ligand. The observed phosphorescence from both complexes is almost identical to that of analogous phosphine-containing systems such as *cis*-[Pt(C≡C-HBC)₂(dppe)], *trans*-[Pt(C≡C-HBC)₂(PPh₃)₂] and *trans*-[Pt(C≡C-Pyr)₂(PBU₃)₂].^[16,30b] The phosphorescence is evidently derived from a ³ππ* excited state located on the extended aromatic chromophore. The effect of extending the π conjugation of the acetylide is to introduce an energetically accessible ³ππ* excited state, localised on the alkynyl moiety, that is lower in energy than ³MMLL/CT [Pt(d)/π(C≡CAr)→π*(N^N)].

Pt^{II} complexes as ¹O₂ sensitisers for DHN photooxidation:

The ability of Pt^{II} complexes **5** (Pyr) and **7** (HBC) to sensitise ¹O₂ production was examined in a series of photooxidation experiments. The long-lived, low-lying triplet excited states (³IL) formed by photoexcitation of **5** and **7** sensitise the conversion of ³O₂ to the highly reactive ¹O₂ species. The model reaction investigated was the oxidation of 1,5-dihydroxynaphthalene

(DHN) to juglone by ¹O₂ generated in situ (Scheme 2), which can be monitored by the reduction in absorption of DHN as it is consumed over the course of the reaction ($\epsilon = 7664 \text{ M}^{-1} \text{ cm}^{-1}$ at $\lambda = 301 \text{ nm}$) and the resulting increase in absorption at $\lambda = 427 \text{ nm}$ due to the formation of juglone ($\epsilon = 3811 \text{ M}^{-1} \text{ cm}^{-1}$).^[24c,47]

For each experiment, an excess of DHN was maintained (5 mol% of photosensitiser relative to DHN), the reaction



Scheme 2. Photooxidation of 1,5-dihydroxynaphthalene (DHN) to juglone.^[45]

mixture irradiated and UV spectra were recorded at 2–10 min intervals over the course of 60 min. The known compounds [Pt(bpy)(C≡CPh)₂] and [Ru(bpy)₃]Cl₂ were employed as reference materials. Each of the compounds measured proved to be photostable under the reaction conditions employed, and this precludes absorption spectral changes due to decomposition or photochemical reaction of the complex.

Relatively efficient photooxidation of DHN is evident from the absorption spectra of **5** and **7** (Figure 7a, b). In

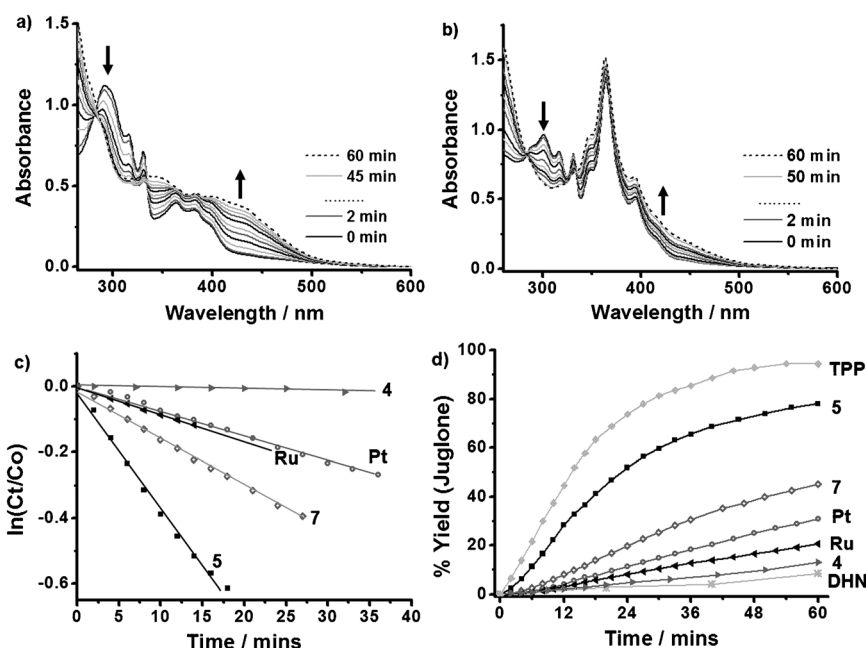


Figure 7. Photooxidation of DHN ($1 \times 10^{-4} \text{ M}$) with Pt^{II} complexes **5** and **7**, [Pt(bpy)(C≡CPh)₂], [Ru(bpy)₃]²⁺ and TPP as ¹O₂ photosensitiser ($5 \times 10^{-6} \text{ M}$) in CH₂Cl₂/CH₃OH (9/1 v/v), irradiated with a halogen bulb lamp (power output: 3 mW cm^{-2}). a) UV/Vis absorption spectral change of DHN with time with **5** as sensitizer. b) Complex **7** as sensitizer. c) Plots of $\ln(C_t/C_0)$ versus irradiation time. d) Plots of chemical yield of juglone versus irradiation time.

contrast, complex **4** (CF₃) behaves quite poorly, as is evident from the marginal changes in absorption with irradiation time (Figure S9, Supporting Information). This may be explained by its poor absorption of visible light and relatively short triplet excited-state lifetime. A quantitative comparison may be achieved by plotting $\ln(C_t/C_0)$ against irradiation time (C_t =DHN concentration at time t , C_0 =initial DHN concentration), the slope of which can be used to derive the pseudo-first-order oxidation rate constants (see Experimental Section). The photooxidation rate with pyrenyl-**5** as sensitizer ($k_{\text{obs}} = 39.3 \times 10^{-3} \text{ min}^{-1}$) is four times higher than that of [Pt(bpy)(C≡CPh)₂] ($k_{\text{obs}} = 9.2 \times 10^{-3} \text{ min}^{-1}$) and is more than half that of the known ¹O₂ sensitiser tetraphenylporphyrin (TPP, $k_{\text{obs}} = 78.6 \times 10^{-3} \text{ min}^{-1}$) under these conditions. Furthermore, the chemical yield of juglone with increasing irradiation time was calculated for each singlet-oxygen photosensitiser (Figure 7d). After 60 min of irradiation time, complex **5** (78%) followed by HBC-**7** (45%) achieved the

Table 4. Photooxidation-related parameters of Pt^{II} complexes **4**, **5** and **7** and reference compounds [Pt(bpy)(C≡CPh)₂], [Ru(bpy)₃]Cl₂ and TPP (CH₂Cl₂/CH₃OH 9/1 v/v, 298 K).

Complex	10 ³ <i>k</i> _{obs} ^[a] [min ⁻¹]	10 ⁷ <i>v</i> _i ^[b] [Mmin ⁻¹]	Φ _Δ ^[c]	Yield [%] ^[d]
4 (CF ₃)	0.29	0.29	0.16	13.0
5 (Pyr)	39.3	39.3	0.35	78.0
7 (HBC)	15.3	15.3	0.23	45.0
[Pt(bpy)(≡Ph) ₂]	9.2	9.2	0.57	29.8
[Ru(bpy) ₃]Cl ₂	7.3	7.3	0.20	20.5
TPP	78.6	78.6	0.62 ^[c]	94.3

[a] Pseudo-first-order rate constant, $\ln(C_i/C_0) = -k_{\text{obs}}t$. [b] Initial rate of DHN consumption, $v_i = k_{\text{obs}}[\text{DHN}]$. [c] Quantum yield of ¹O₂ generation with TPP (Φ_Δ = 0.62) as reference.^[49,50] [d] Yield of juglone after 60 min of reaction time.

highest conversion of DHN to juglone of the studied systems (Table 4).

As a final comparison, the singlet-oxygen quantum yields of the Pt^{II} complexes were calculated by using the known singlet-oxygen photosensitiser TPP as reference and 1,3-diphenylisobenzofuran (DPBF) as ¹O₂ scavenger (see Experimental Section).^[48] Complexes **5** and **7** showed ¹O₂ quantum yields which were half and one-third, respectively, of that of TPP, and reveal an efficient triplet–triplet energy-transfer process in both cases and correspond to the DHN photooxidation results. Interestingly, the Pt^{II} reference complex essentially matched the singlet-oxygen quantum efficiency of TPP itself, and this reveals a highly efficient photosensitisation process when DPBF is employed as ¹O₂ scavenger. In contrast, photooxidation of DHN is only reasonably efficient. As the conversion of DHN to juglone is proposed to involve initial trapping of ¹O₂ by DHN to form an adduct (assumed to be the rate-determining step) followed by dehydration to form juglone, it would appear that formation of the adduct inhibits further DHN photooxidation.^[47] This suggests the involvement of one or more additional processes unrelated to ¹O₂, which makes the kinetic analysis significantly more complicated. DPBF appears to be a more suitable substrate for ¹O₂ photoreaction sensitised by [Pt(bpy)(≡Ph)₂] and shows an impressive ¹O₂ quantum efficiency.

Conclusions

A series of novel [Pt(N[^]N)(C≡CR)₂] complexes containing a polyarylated bipyridine have been synthesised. The electronic character, steric bulk and π-electronic delocalization of substituents on the acetylide co-ligands were systematically varied (R = *tert*-butyl, trifluoromethyl, pyrene, hexaphenylbenzene, HBC). The complexes were characterised by variable-temperature NMR and infrared spectroscopy, mass spectrometry, elemental analysis and single-crystal X-ray crystallography. The variable-temperature NMR experiments supported the conclusion that the presence of a polyarylated bipyridine imposes considerable steric strain within the molecules and affects markedly the rotational freedom of one or more of the *tert*-butylphenyl rings in complexes **3**–

7. The single-crystal X-ray structure of **3** strongly points to an intramolecular nature of these interactions.

The opto-electronic character of the complexes was explored by UV/Vis absorption spectroscopy, cyclic voltammetry and photoluminescence studies. The lowest-energy absorption and emission maxima were red-shifted with increasing electronic donicity of the acetylide ligands. Complexes **3**, **4** and **6** display broad and increasingly red-shifted emission profiles with lifetimes in the microsecond region (298 K, in the solid state and in solution). This, and the dependence of the Pt^{II} oxidation potential on the nature of the acetylide, suggested that both the C≡CR π and the Pt 5d orbitals participate in the HOMO of these complexes. The emissive excited states were assigned as ³MMLL/CT [Pt(5d)/π(C≡CR) → π*(N[^]N)]. In contrast the emission from complexes **5** and **7**, which have π-conjugated platforms from their acetylide co-ligands, was assigned as [³ππ*(C≡CR)]. These emissions had extended excited-state lifetimes and were characteristic of their appended polyaromatic chromophores. At 298 K, complexes **5** and **7** exhibit high-energy fluorescence due to their respective PAH segments, but at 77 K complex **5** shows only ³ππ* emission, which reveals efficient intersystem crossing from singlet to triplet emissive excited states. Complex **5** also shows a notable concentration dependence attributed to aggregation of the pyrenyl PAH fragments. The properties of **5** and **7** are consistent with an energetically accessible ³ππ* state that is localized on the acetylide and lower in energy than the ³MMLL/CT state.

The triplet excited states of complexes **5** and **7** were shown to be sufficiently long lived to effect the sensitisation of ¹O₂, an effect shown by subsequent photooxidation of DHN present in situ. In contrast, the excited state of **4** is insufficiently long lived to afford an efficient conversion process. The singlet-oxygen quantum yield of pyrenyl complex **5** and, even more effectively, the Pt complex employed as a reference, namely, [Pt(bpy)(C≡CPh)₂], are of a similar order of magnitude to that of the known and readily utilised reference photosensitiser tetraphenylporphyrin.

This series of complexes allowed us to investigate the photophysical effects of varying the steric bulk and electronic demand of acetylide co-ligands in Pt^{II} complexes with the same diimine structural motif. The novelty of these complexes is derived from their inherent asymmetry, whereby a polyarylated bipyridine with several potential coordination modes partially envelops a photoactive metal centre. The detailed investigation of such structure–property relationships and efforts to exploit triplet excited states for real-world purposes are fundamental to the quest for optimised novel systems for opto-electronic and photosensitisation applications.

Experimental Section

Electronic Supplementary Information (ESI) available: For experimental details, including synthesis, characterisation and X-Ray crystallography, see the Supporting Information.

Acknowledgements

We thank Drs. John O'Brien, Manuel Ruether and Martin Feeney for technical assistance and Dr. Thomas McCabe for additional X-ray crystallography. This material is based upon works supported by the Irish Research Council (Embark) (IRCSET) (D.N.) and the European Union Framework 6 Programme (EU FP6) (MKTD-CT-2004-014472) (B.G.) and SFI 10/IN.1/12974 and STTF-11.

- [1] U. M. Wiesler, A. J. Berresheim, F. Morgenroth, G. Lieser, K. Müllen, *Macromolecules* **2001**, *34*, 187–199.
- [2] M. Schlupp, T. Weil, A. J. Berresheim, U. M. Wiesler, J. Bargon, K. Müllen, *Angew. Chem.* **2001**, *113*, 4124–4129; *Angew. Chem. Int. Ed.* **2001**, *40*, 4011–4015.
- [3] P. Du, J. Schneider, W. W. Brennessel, R. Eisenberg, *Inorg. Chem.* **2008**, *47*, 69–77.
- [4] a) T. Weil, E. Reuther, K. Müllen, *Angew. Chem.* **2002**, *114*, 1980–1984; *Angew. Chem. Int. Ed.* **2002**, *41*, 1900–1904; b) P. Schlichting, B. Duchscherer, G. Seisenberger, T. Basche, C. Brauchle, K. Müllen, *Chem. Eur. J.* **1999**, *5*, 2388–2395.
- [5] G. Kodis, Y. Terazono, P. A. Liddell, J. Andreasson, V. Garg, M. Hamburger, T. A. Moore, A. L. Moore, D. Gust, *J. Am. Chem. Soc.* **2006**, *128*, 1818–1827.
- [6] a) M. C. Haberecht, J. M. Schnorr, E. V. Andreitchenko, C. G. Clark, Jr., M. Wagner, K. Müllen, *Angew. Chem.* **2008**, *120*, 1686–1691; *Angew. Chem. Int. Ed.* **2008**, *47*, 1662–1667; b) T. Qin, J. Ding, L. Wang, M. Baumgarten, G. Zhou, K. Müllen, *J. Am. Chem. Soc.* **2009**, *131*, 14329–14336.
- [7] S. Brydges, L. E. Harrington, M. J. McGlinchey, *Coord. Chem. Rev.* **2002**, *233–234*, 75–105.
- [8] H. P. Dijkstra, P. Steenwinkel, D. M. Grove, M. Lutz, A. L. Spek, G. Van Koten, *Angew. Chem.* **1999**, *111*, 2321–2324; *Angew. Chem. Int. Ed.* **1999**, *38*, 2185–2188.
- [9] a) M. Müller, C. Kubel, K. Müllen, *Chem. Eur. J.* **1998**, *4*, 2099–2109; b) S. M. Draper, D. J. Gregg, R. Madathil, *J. Am. Chem. Soc.* **2002**, *124*, 3486–3487; c) D. J. Gregg, E. Bothe, P. Hofer, P. Passaniti, S. M. Draper, *Inorg. Chem.* **2005**, *44*, 5654–5660.
- [10] a) M. A. Baldo, D. F. O'Brien, Y. You, A. Shoustikov, S. Sibley, M. E. Thompson, S. R. Forrest, *Nature* **1998**, *395*, 151–154; b) R. C. Evans, P. Douglas, C. J. Winscom, *Coord. Chem. Rev.* **2006**, *250*, 2093–2126.
- [11] K. D. Ley, K. S. Schanze, *Coord. Chem. Rev.* **1998**, *171*, 287–307.
- [12] V. M. Miskowski, V. H. Houlding, *Inorg. Chem.* **1989**, *28*, 1529–1533.
- [13] C. W. Chan, L. K. Cheng, C. M. Che, *Coord. Chem. Rev.* **1994**, *132*, 87–97.
- [14] M. Hissler, W. B. Connick, D. K. Geiger, J. E. McGarrah, D. Lipa, R. J. Lachicotte, R. Eisenberg, *Inorg. Chem.* **2000**, *39*, 447–457.
- [15] a) C. E. Whittle, J. A. Weinstein, M. W. George, K. S. Schanze, *Inorg. Chem.* **2001**, *40*, 4053–4062; b) S. C. Chan, M. C. W. Chan, Y. Wang, C. M. Che, K. K. Cheung, N. Zhu, *Chem. Eur. J.* **2001**, *7*, 4180–4190.
- [16] I. E. Pomestchenko, C. R. Luman, M. Hissler, R. Ziessel, F. N. Castellano, *Inorg. Chem.* **2003**, *42*, 1394–1396.
- [17] J. E. McGarrah, R. Eisenberg, *Inorg. Chem.* **2003**, *42*, 4355–4365.
- [18] a) P. Du, K. Knowles, R. Eisenberg, *J. Am. Chem. Soc.* **2008**, *130*, 12576–12577; b) P. Jarosz, P. Du, J. Schneider, S.-H. Lee, D. McCamant, R. Eisenberg, *Inorg. Chem.* **2009**, *48*, 9653–9663.
- [19] a) W. Lu, M. C. W. Chan, N. Zhu, C. M. Che, Z. He, K. Y. Wong, *Chem. Eur. J.* **2003**, *9*, 6155–6166; b) J. Ni, Y. H. Wu, X. Zhang, B. Li, L. Y. Zhang, Z. N. Chen, *Inorg. Chem.* **2009**, *48*, 10202–10210.
- [20] E. C. H. Kwok, M. Y. Chan, K. M. C. Wong, W. H. Lam, V. W. W. Yam, *Chem. Eur. J.* **2010**, *16*, 12244–12254.
- [21] K. M.-C. Wong, W.-S. Tang, B. W.-K. Chu, N. Zhu, V. W.-W. Yam, *Organometallics* **2004**, *23*, 3459–3465.
- [22] Y. Li, A. Y.-Y. Tam, K. M.-C. Wong, W. Li, L. Wu, V. W.-W. Yam, *Chem. Eur. J.* **2011**, *17*, 8048–8059.
- [23] X. Wang, S. b. Goeb, Z. Ji, N. A. Pogulaichenko, F. N. Castellano, *Inorg. Chem.* **2011**, *50*, 705–707.
- [24] a) H. Sun, H. Guo, W. Wu, X. Liu, J. Zhao, *Dalton Trans.* **2011**, *40*, 7834–7841; b) H. Guo, Q. Li, L. Ma, J. Zhao, *J. Mater. Chem.* **2012**, *22*, 15757–15768; c) J. Sun, J. Zhao, H. Guo, W. Wu, *Chem. Commun.* **2012**, *48*, 4169–4171; d) J. Zhao, S. Ji, W. Wu, W. Wu, H. Guo, J. Sun, H. Sun, Y. Liu, Q. Li, L. Huang, *RSC Adv.* **2012**, *2*, 1712–1728.
- [25] M. C. DeRosa, R. J. Crutchley, *Coord. Chem. Rev.* **2002**, *233–234*, 351–371.
- [26] M. Vrábel, M. Hocek, L. Havran, M. Fojta, I. Votruba, B. Klepešová, R. Pohl, L. Rulíšek, L. Zendllova, P. Hobza, I. H. Shih, E. Mabery, R. Mackman, *Eur. J. Inorg. Chem.* **2007**, 1752–1769.
- [27] a) D. J. Cárdenas, A. M. Echavarren, M. C. Ramírez de Arellano, *Organometallics* **1999**, *18*, 3337–3341; b) J. Ding, D. Pan, C. H. Tung, L. Z. Wu, *Inorg. Chem.* **2008**, *47*, 5099–5106; c) S. Diring, P. Retailleau, R. Ziessel, *J. Org. Chem.* **2007**, *72*, 10181–10193; d) P. Wu, E. L. M. Wong, D. L. Ma, G. S. M. Tong, K. M. Ng, C. M. Che, *Chem. Eur. J.* **2009**, *15*, 3652–3656; e) M. Y. Yuen, S. C. F. Kui, K. H. Low, C. C. Kwok, S. S. Y. Chui, C. W. Ma, N. Zhu, C. M. Che, *Chem. Eur. J.* **2010**, *16*, 14131–14141; f) A. Zucca, G. L. Petretto, M. L. Cabras, S. Stoccoro, M. A. Cinellu, M. Manassero, G. Minghetti, *J. Organomet. Chem.* **2009**, *694*, 3753–3761.
- [28] J. Schneider, P. Du, X. Wang, W. W. Brennessel, R. Eisenberg, *Inorg. Chem.* **2009**, *48*, 1498–1506.
- [29] G. W. V. Cave, F. P. Fanizzi, R. J. Deeth, W. Errington, J. P. Rourke, *Organometallics* **2000**, *19*, 1355–1364.
- [30] a) F. A. Murphy, S. M. Draper, *J. Org. Chem.* **2010**, *75*, 1862–1870; b) D. Nolan, B. Gil, F. A. Murphy, S. M. Draper, *Eur. J. Inorg. Chem.* **2011**, 3248–3256; c) C. M. Ollagnier, D. Nolan, C. M. Fitchett, S. M. Draper, *Inorg. Chem. Commun.* **2007**, 1045–1048.
- [31] C. J. Adams, S. L. James, X. Liu, P. R. Raithby, L. J. Yellowlees, *J. Chem. Soc. Dalton Trans.* **2000**, 63–67.
- [32] a) S. Diring, P. Retailleau, R. Ziessel, *Tetrahedron Lett.* **2007**, *48*, 8069–8073; b) Q. Y. Cao, W. F. Fu, X. L. Zhao, *Acta Crystallogr. Sect. E* **2005**, *61*, 427–429; c) A. Hofmann, L. Dahlenburg, R. Van Eldik, *Inorg. Chem.* **2003**, *42*, 6528–6538.
- [33] D. J. Gregg, C. M. A. Ollagnier, C. M. Fitchett, S. M. Draper, *Chem. Eur. J.* **2006**, *12*, 3043–3052.
- [34] P. K. M. Siu, S. W. Lai, W. Lu, N. Zhu, C. M. Che, *Eur. J. Inorg. Chem.* **2003**, 2749–2752.
- [35] N. I. Nijegorodov, W. S. Downey, *J. Phys. Chem.* **1994**, *98*, 5639–5643.
- [36] V. M. Miskowski, V. H. Houlding, C. M. Che, Y. Wang, *Inorg. Chem.* **1993**, *32*, 2518–2524.
- [37] a) Z. Ji, Y. Li, W. Sun, *Inorg. Chem.* **2008**, *47*, 7599–7607; b) Z. Ji, A. Azenkeng, M. Hoffmann, W. Sun, *Dalton Trans.* **2009**, 7725–7733.
- [38] a) S. Fernández, J. Forniés, B. Gil, J. Gómez, E. Lalinde, *Dalton Trans.* **2003**, 822–830; b) A. Klein, J. Van Slageren, S. Zalis, *Eur. J. Inorg. Chem.* **2003**, 1917–1928.
- [39] S. D. Cummings, R. Eisenberg, *J. Am. Chem. Soc.* **1996**, *118*, 1949–1960.
- [40] C. B. Blanton, Z. Murtaza, R. J. Shaver, D. P. Rillema, *Inorg. Chem.* **1992**, *31*, 3230–3235.
- [41] E. Bircckner, U. W. Grummt, A. H. Goeller, T. Pautzsch, D. A. M. Egbe, M. Al-Higari, E. Klemm, *J. Phys. Chem. A* **2001**, *105*, 10307–10315.
- [42] P. Chen, T. J. Meyer, *Chem. Rev.* **1998**, *98*, 1439–1477.
- [43] K. Y. Kim, S. Liu, M. E. Kose, K. S. Schanze, *Inorg. Chem.* **2006**, *45*, 2509–2519.
- [44] B. El Hamaoui, F. Laquai, S. Balushev, J. Wu, K. Müllen, *Synth. Met.* **2006**, *156*, 1182–1186.
- [45] D. Pant, U. C. Tripathi, G. C. Joshi, H. B. Tripathi, D. D. Pant, *J. Photochem. Photobiol. A* **1990**, *51*, 313–325.
- [46] T. Hard, P. Fan, D. R. Kearns, *Photochem. Photobiol.* **1990**, *51*, 77–86.
- [47] S.-y. Takizawa, R. Aboshi, S. Murata, *Photochem. Photobiol. Sci.* **2011**, *10*, 895–903.

- [48] Y. Cakmak, S. Kolemen, S. Duman, Y. Dede, Y. Dolen, B. Kilic, Z. Kostereli, L. T. Yildirim, A. L. Dogan, D. Guc, E. U. Akkaya, *Angew. Chem.* **2011**, *123*, 12143–12147; *Angew. Chem. Int. Ed.* **2011**, *50*, 11937–11941.
- [49] J. W. Arbogast, A. P. Darmany, C. S. Foote, F. N. Diederich, R. L. Whetten, Y. Rubin, M. M. Alvarez, S. J. Anz, *J. Phys. Chem.* **1991**, *95*, 11–12.
- [50] a) L. Huang, X. Yu, W. Wu, J. Zhao, *Org. Lett.* **2012**, *14*, 2594–2597;
b) L. Liu, D. Huang, S. M. Draper, X. Yi, W. Wu, J. Zhao, *Dalton Trans.*, DOI: 10.1039/C3DT50496D.

Received: February 26, 2013

Revised: July 2, 2013

Published online: September 24, 2013